Department of Pharmaceutics[1], China Pharmaceutical University, Nanjing, China; School of Pharmacy[2], University of Auckland, Auckland, New Zealand; Atherosclerosis Research Centre[3], Nanjing Medical University, Nanjing, China

Tanshinone IIA-loaded reconstituted high density lipoproteins: Atherosclerotic plaque targeting mechanism in a foam cell model and pharmacokinetics in rabbits

Wenli Zhang[1], Jin Li[1], Jianping Liu[1], Zimei Wu[2], Yiming Xu[3], Ji Wang[1]

Received April 18, 2011, accepted May 16, 2011

Jianping Liu, Department of Pharmaceutics, China Pharmaceutical University, Nanjing, 210009, PR China
liujianpingljp@hotmail.com
Zimei Wu, School of Pharmacy, University of Auckland, Auckland, New Zealand
z.wu@auckland.ac.nz

Pharmazie 67: 324–330 (2012) *doi: 10.1691/ph.2012.1055*

Spherical and discoidal tanshinone IIA-loaded reconstituted high density lipoproteins (TA-rHDL) with different formulations and techniques were prepared and characterized. The targeting mechanism was investigated using a foam cell model. Pharmacokinetics of four TA-rHDL formulations with or without apolipoproteins (apos) after a single dose intravenous injection to rabbits has been studied. The results showed that the sizes of spherical and discoidal TA-rHDL increased after coupling with apos from 55.38 nm to 157.26 nm, 61.03 nm to 166.19 nm, and zeta potential decreased from −29.2 mV to −35.4 mV, −5.2 mV to −11.82 mV, respectively. The results of circular dichroic spectroscopy indicated variations of apos in protein secondary structure after binding with lipids. Phagocytosis tests demonstrated that the spherical TA-rHDL had a targeting effect for foam cells through the scavenger receptor-BI and CE-TG interchange with TG-rich lipoproteins pathway under cholesteryl ester transfer protein. Discoidal TA-rHDL could reconstruct to spheres and target *via* a similar route as TA-rHDL spheres, showing a higher targeting efficiency. *In vivo* experiments showed that areas under the plasma level-time curve (AUC) of TA increased as a function of spherical and discoidal rHDL, which were 4 and 13 times more than that of TA suspensions, respectively. Spherical and discoidal TA-rHDL had long circulating times in blood with mean residence time (MRT) of 15.874 and 18.956 h, respectively, compared to 1.802 h of TA suspensions, 14.190 h of spherical TA-rHDL without apos and 15.071 of discoidal TA-rHDL without apos. The distribution volume of spherical TA-rHDL was 2.143 and 1.552 times as that of discoidal TA-rHDL and TA suspensions, respectively. In conclusion, TA-rHDL may be a long-circulating, healthy and potentially targeted carrier for delivering lipophilic cardiovascular drugs.

1. Introduction

Tanshinone IIA (TA), one of the liposoluble active components extracted from the root of *Salvia miltiorrhiza Bunge*, is an effective cardiovascular agent which can dilate coronary arteries and increase myocardial contractility (Zhao et al. 1996). However, the majority of orally administered drugs has a low bioavailability due to the negligible solubility of tashinone IIA in water and its first pass metabolism (Hao et al. 2007). In addition, tashinone IIA has a very short half-life (1∼2 h) which limits its therapeutic effects. It decomposes under light and high temperature (> 80 °C), resulting in a loss of activity (Su et al. 1997). Recently, a number of strategies have been employed to address these issues, e.g., polymeric nanoparticles (Li et al. 2008), emulsions (Liang et al. 2008), microemulsions (Li et al. 2007), proliposomes (Chu et al. 2002), nanoparticles (Liang et al. 2007) and so on.

In our previous studies, tanshinone IIA-loaded solid lipid nanoparticles (TA-SLN) have been developed as a carrier system for its superiorities with manageable burst effect issue, prolonged circulation time, as well as increased AUC (Liu et al. 2005; Zhang et al. 2009). Currently, Schöler et al. (2002) have reported that the nature of the lipid matrix and concentration of nanoparticles influenced their cytotoxic effects on macrophages. As known to all, a variety of different emulsifiers have been used for the preparation of SLN dispersions, including bile salts, poloxamers, and other ionic and nonionic surfactants which can induce irritative, hemolytic, or sensitizing action (Bunjes et al. 2003; Han et al. 2008; Joshi et al. 2008). Furthermore, lipids used in SLN such as glycerin monostearate, triglyceride and stearic acid were not beneficial to cardiovascular patients. Animal and clinical studies have provided convincing evidence that the metabolism of lipid was related to the incidence of coronary heart disease (Kontush and Chapman 2006). Therefore, lipid matrices and surfactant should be even more carefully chosen and tested for later intravenous use when a cardiovascular agent is encapsulated in lipid particles.

Abbreviations: rHDL, reconstituted high density lipoproteins; TA-rHDL, Tanshinone IIA-loaded reconstituted high density lipoproteins; CE, cholesterol esters; TG, triglycerides; RCT, reverse cholesterol transportation; Apo, apolipoprotein; LCAT, lecithin:cholesterol acyl transferase; SR-BI, scavenger receptor-BI; DLS, dynamic light scattering; CD, circular dichroism; ox-LDL, oxidized low density lipoproteins; CETP, cholesteryl ester transfer protein; VLDL, very low density lipoproteins.

Table 1: Zeta potential values and average diameter of spherical and discoidal TA-rHDL (n = 3, mean ± SD)

Formulation		Zeta potential (mV)		Size (nm)	
		Before incubation	After incubation	Before incubation	After incubation
Spherical	TA-rHDL	−29.20 ± 0.15	−35.4 ± 0.10	55.38 ± 2.5	157.26 ± 5.6
Discoidal	TA-rHDL	−5.20 ± 0.08	−11.82 ± 0.15	61.03 ± 3.3	166.19 ± 5.3

It has been well established that high-density lipoproteins (HDL) play a protective role against the development of cardiovascular diseases (Linsel-Nitschke and Tall 2005) due to their anti-atherogenic and anti-inflammatory properties (Barter et al. 2004). Natural HDL have a Stoke's diameter of 5–17 nm (Assmann and Nofer 2003) and exist in two different forms: one is in spherical shape, the other is discoidal. The former has a hydrophobic core of triglycerides (TG) and cholesterol esters (CE) covered with a monolayer of phospholipids in which apolipoprotein (apos) are embedded (Ajees et al. 2006; Libby 2008; Thomas et al. 2008). The latter consists of only apos and lipids (phospholipid and cholesterol). The most abundant apo in HDL is apoA-I, a highly α-helical, 28.3 KDa polypeptide, taking up approximately 70% of the HDL protein mass (Vaisar et al. 2007). Acting in conjunction with lecithin:cholesterol acyl transferase (LCAT) which converts free cholesterol to cholesteryl ester, modulated by many factors, nascent discoidal HDL are converted and yield spherical HDL through remodeling the internal structure (Pownall and Gotto 1992).

Since apoA-I can interact with specific receptors such as scavenger receptor-BI (SR-BI) in liver, tumour and steroid-producing tissues. In the past decades, reconstituted HDL (rHDL) have been investigated as a targeting delivery vehicle for many anti tumour and liver disease drugs (Lou et al. 2005; McConathy et al. 2008; Feng et al. 2008). Besides, apoA-I can promote cellular cholesterol efflux, bind lipids and activate lecithin:cholesterol acyl transferase (LCAT), together with other apos such as apoA-II and apoE, play a principal active role in HDL-therapy of coronary artery disease (Saito et al. 2004; Song et al. 2009). Therefore, by using rHDL, it is possible to deliver a lipophilic cardiovascular drug and simultaneously providing therapeutic effects of the carrier.

Recently, there is growing evidence showing the targeting effect of rHDL for atherosclerotic plaque. Skajaa et al. (2010) have found that iron oxide core-HDL particles were able to circulate as single entities and enter the plaque sites individually, in a similar manner as native HDL *in vivo*. Atherosclerotic lesions are characteristic of many lipid-laden "foam cells" (Bobryshev 2006), which are derived from the monocytes that invade the intima of lesion-prone areas in arteries and consequently become phagocytic and accumulate lipid. So far, the mechanisms by which the rHDL target atherosclerosis plaque have not been defined, neither have drug-loaded rHDL.

The present study was done to develop a drug-loaded rHDL system with dual roles of targeting the drug to atherosclerosis plaque and simultaneously providing a therapeutic effect of the carrier. Tanshinone IIA (TA), a well-known traditional Chinese medicine for treating atherosclerosis, was selected as a model drug. In a previous study (Zhang et al. 2010a), TA-NLC (tanshinone IIA loaded nanostructured lipid carriers) was reconstituted only with lipid components of native HDL, which could compete for apos of native HDL *in vitro*. Given the bionic function of apos in cardiovascular therapy, in this study, TA-loaded rHDL (TA-rHDL) using apos as an important component have been constituted and characterized. The exact structures of TA-rHDL have been investigated and will be reported elsewhere. This study aimed to investigate the targeting effect of

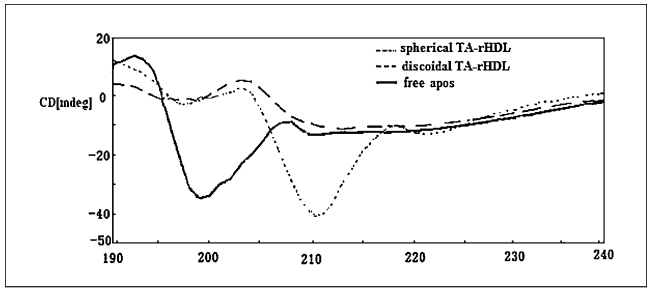

(A)

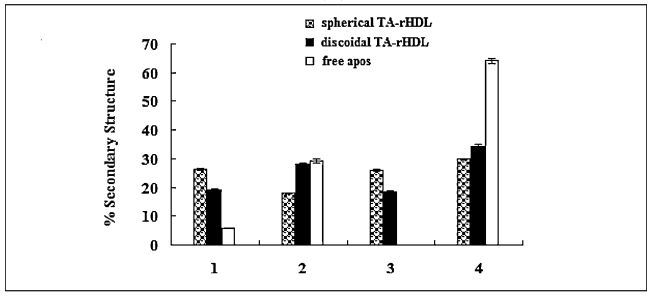

(B)

Fig. 1: Circular dichroic spectra (A) and percentages of secondary structure (B) of free apos, spherical and discoidal TA-rHDL.

TA-rHDL with two different structures using an *in vitro* foam cell model mimicking the atherosclerosis plaque and the differences in pharmacokinetics of free TA and TA-rHDL with and without apolipoprotein coating in rabbits, evaluating the potential of using rHDL as a parenteral delivery carrier for poorly water soluble cardiovascular drugs.

2. Investigations, results and discussion

2.1. Size and zeta potential

Table 1 shows that the size of spherical and discoidal TA-rHDL were similar ($p > 0.05$) before (~60 nm) and after incubation with apos (~160 nm). The increase in particle size after incubation may result from a more hydrophilic surface (Ogino et al. 2010) and confirm the formation of a complex with the lipid particles surrounded by the apos in the structure. In addition, the coupling of apos also influenced the zeta potential of the particles. The increase of the negative charge observed in both spherical and discoidal TA-rHDL after incubation indicated that apos, being amphipathic and negative-charged at pH = 8.0, have been anchored on the surface of lipid particles.

2.2. Secondary structure of apolipoproteins

Circular dichroism (CD) was used to estimate the average secondary stucture content of apolipoproteins in the lipid-bound and free form. As seen from Fig. 1, the CD spectrum of spherical TA-rHDL was characterized by a high overall ellipticity with negative values at 209 nm and 222 nm, suggesting a large amount of α-helix. The spectrum of discoidal TA-rHDL with negative

value positions was similar to that of the spherical. Besides, the higher value of ellipticity at 222 nm suggested that discoidal TA-rHDL had less α-helix than spherical TA-rHDL. The typical absorption peaks of β-structure in free apos were observed with a positive value at 193 nm and a negative value at 217 nm. Seen from the bar graph, the content of α-helix increased from 5% to more than 20% after binding with lipid. In contrast, lipid-bound apos in either discoidal or spherical TA-rHDL presented less β-structure and random coil than free apos. The conformational transition from random coil to α-helix upon lipid-binding is thought to provide the energetic source to drive the lipid interaction of apos (Massey and Gotto 1979). The results of CD spectrum proved the binding of lipid with apos, which is consistent with that reported by McGuire et al. (1996).

2.3. Phagocytosis tests

The results in Fig. 2 show that apos in spherical TA-rHDL significantly increased their uptake by foam cell irrespective of the VLDL in the culture medium (a *vs* b; c *vs* d). In addition, the uptake of spherical TA-rHDL without VLDL by foam cells was higher than that by macrophages (d *vs* e). Results also show that the presence of VLDL had significantly increased phagocytosis uptake of the spherical TA-rHDL by foam cells (b *vs* d). In contrast, the drug uptake in nanoparticles by foam cells was weakened by VLDL in the medium (a *vs* c).

There were probably two kinds of targeting mechanism for spherical TA-rHDL. One was the direct apoA-I act on the receptors in the foam cells such as ABCA1 protein, ABCG-I and SR-BI (Collet et al. 1999; Fitzgerald et al. 2010; Hiltunen et al. 1998; Zannis et al. 2006), which was inferred from the significantly increased drug uptake of spherical TA-rHDL by foam cells after incubation with apos. The other was indirect targeting act through VLDL after structure remodeling of TA-rHDL. VLDL had remarkably increased uptake of spherical TA-rHDL by transfected foam cells expressing CETP, which implied that remodeling of spherical TA-rHDL may have contributed to specific targeting of TA-rHDL. During the remodeling process, spherical TA-rHDL may undergo a CE-TG interchange with VLDL under the action of CETP and lipase (Collet et al. 1999). Then the drug loaded in VLDL was taken up via the VLDL receptors by foam cells. It was reported that VLDL and SR-BI receptors in foam cells are related to the cellular uptake of native HDL, SR-BI receptors for macrophages (Mahley and Innerarity 1983). It was also noted that the uptake of spherical TA-rHDL without VLDL by foam cells was higher than that by macrophages (d *vs* e). This coincided with the findings (Hiltunen et al. 1998) that SR-BI and VLDL receptors in atherosclerotic lesions were both highly induced during cholesterol feeding to normal rabbits, and VLDL receptors upgraded faster initially. In contrast, the drug uptake in the lipid cores by foam cells was weakened by VLDL in the medium (a *vs* c), which may result from a competitive effect of VLDL with their receptors.

In contrast to the spherical TA-rHDL, there was no further increase in discoidal TA-rHDL uptake when VLDL were added (g *vs* h), however, boosted after exposure to LCAT (h *vs* i) as reported by other researchers (Collet et al. 1999; Francone et al. 1989). Furthermore, the uptake of the discoidal TA-rHDL by the foam cells was higher than that of spherical TA-rHDL under the same conditions (h *vs* b, g *vs* d). Two important conclusions may be drawn from aforementioned phenomena: (1) Discoidal TA-rHDL may undergo a structure transformation from bilayer-discs to spheres□then deliver drug to foam cells in a similar pathway as spherical TA-rHDL, which offers an explanation for the LCAT dependent increase of discoidal TA-rHDL uptake. Furthermore, it can be concluded that the restructured spherical TA-rHDL from discoidal TA-rHDL were more susceptible for internalization than artifical TA-rHDL spheres (h *vs* b). (2) Discoidal TA-rHDL without VLDL and LCAT were speculated to be able to maintain the polar lipid bilayers, as in cell membranes (Phillips et al. 1997), therefore they were taken up more easily compared to spherical TA-rHDL (g *vs* d).

Also, the uptake of both spherical and discoidal TA-rHDL decreased with time of incubation. The likely explanation is that cells phagocytozing plenty of TA-rHDL had floated in the DMEM medium after 1 h and were washed away by D-PBS (Feng et al. 2005).

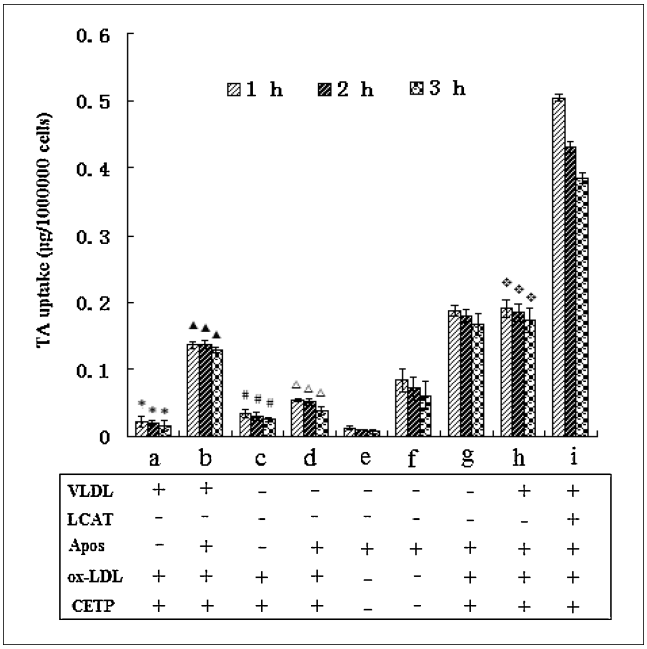

Fig. 2: Drug uptake of nanoparticles (a and c), spherical TA-rHDL (b and d) and discoidal TA-rHDL with (i) or without (g and h) LCAT by foam cells expressing CETP in the presence (a, b, h and i) or absence (c, d and g) of VLDL; spherical (e) and discoidal (f) TA-rHDL by macrophages in the absence of VLDL after different incubation periods. + ox-LDL means foam cell. – ox-LDL means macrophages. Results (mean ± SD, n = 3) are expressed as the amount of TA phagocytozed with respect to 1 000 000 cells. Statistical significances ($p < 0.05$) between ∗: a and c; ▲: b and d; #: c and d; ⌜: d and e; ◇: h and i. Table shows different conditions for phagocytosis test.

2.4. Pharmacokinetic analysis

The pharmacokinetic data of five formulations (e.g. TA suspension, spherical TA-rHDL with or without apos, discoidal TA-rHDL with or without apos) were processed using statistical moment methods and the results are shown in Table 2. Their plasma concentrations of TA *vs* time obtained after injection are given in Fig. 3 and Fig. 4.

As can be seen from Figs. 3 and 4, TA was still present 24 h after injection of TA-rHDL either with or without apos. However, no drug was detectable 4 h after intravenous injection of TA suspensions. As shown in Table 2 MRT of the rHDL formulations were longer than that of TA suspensions, indicating a sustained release as the function of rHDL, liposomes or nanoparticles. AUC of TA incorporated in discoidal and spherical TA-rHDL, irrespective of binding with apos, increased 4 and 13 times compared to TA suspensions. The small total body clearance rates (CL) for both TA-rHDL without and with apos indicated that TA incorporated in these particles removed slowly from circulating system compared to TA suspensions.

For spherical structure, after coupling with apos, TA-rHDL showed prolonged MRT and enlarged distribution volume (V_d) relative to nanoparticles (spherical TA-rHDL without apos)

Table 2: Pharmacokinetic parameters of TA in rabbits after i.v. administration of TA suspensions, nanoparticles, liposomes, spherical and discoidal TA-rHDL (n = 6, mean ± S.D.)

Formulations	CL/L·kg^{-1}·h^{-1}	V_d/L·kg^{-1}	$AUC_{0\text{-}t}$/μg·h·mL^{-1}	MRT/h
TA				
Suspensions	11.250 ± 1.392*	20.27 ± 4.275*	0.038 ± 0.004*	1.802 ± 0.294*
Nanoparticles	1.974 ± 0.271	28.012 ± 4.119	0.195 ± 0.012	14.190 ± 2.038
Spherical TA-rHDL	1.982 ± 0.134	31.465 ± 6.061▲▲	0.193 ± 0.061	15.874 ± 1.314▲▲
Liposomes	1.007 ± 0.236	15.180 ± 1.103	0.430 ± 0.096	15.071 ± 1.090
Discoidal TA-rHDL	0.774 ± 0.059**	14.680 ± 1.046ΔΔ	0.537 ± 0.110**	18.956 ± 1.257**

*$p < 0.05$ TA suspensions vs other formulations
▲▲$p < 0.05$ spherical TA-rHDL vs nanoparticles
*$p < 0.05$ discoidal TA-rHDL vs liposomes
ΔΔ$p < 0.05$ discoidal TA-rHDL vs spherical TA-rHDL

($p < 0.05$). However, their AUC and body clearances did not show significant differences. The prolonged MRT is ascribed to the coupling of apos in the TA-rHDL, which could not trigger immunological responses and reduced uptake by macrophages as also reported (Herbert et al. 1984; Rensen et al. 2001). The enlarged V_d for spherical TA-rHDL may be explained by a possibly apoA-I mediated targeting effect (Feng et al. 2008) which increased drug concentration in peripheral issues.

For discoidal structure, TA-rHDL also showed a longer MRT compared to liposomes (discoidal TA-rHDL without apos) ($p < 0.05$) like the spherical. Consistent with the slower CL of TA-rHDL, a bigger AUC than in liposomes ($p < 0.05$) was observed. However, the V_d of discoidal TA-rHDL and liposomes were similar to that of TA suspensions, indicating their poor capacity to distribute to peripheral issues.

As seen from the curves in Fig. 3 and 4, both spherical and discoidal TA-rHDL displayed a multi-peak phenomenon. For spherical TA-rHDL, peaks at 3 and 12 h were observed, which may arise from a multistage release process of TA-rHDL. Since dynamic association/dissociation equilibrium existed between apo-bound (TA-rHDL) and free particles (nanoparticles), the dissociation of nanoparticles from apos might cause the aforementioned multistage release, therefore, the concentration for TA-rHDL suddenly increased. Inferred from the peak time, this phenomenon for spherical TA-rHDL can also be explained by "enterohepatic circulation" (Marier et al. 2002). It was reported (Li et al. 2006) that TA was predominantly excreted into bile. Given the probably hepatic targeting effect of rHDL as reported (Feng et al. 2008), this pathway of biliary excretion may be enhanced, which would induce re-absorption of TA from the intestinal tract. As for discoidal TA-rHDL, a second peak at 20 min can also be explained by dynamic association/dissociation equilibrium. In addition, the second peak may be a sudden drug release or leakage from discoidal TA-rHDL during interaction with endogenous matter such as native HDL (Scherphof et al. 1978) and LCAT (Angelin et al. 2002), which was also proved by the lower V_d than that of TA suspensions. Therefore, we conjectured the discoidal rHDL were easily destroyed in circulation systems and has poor capacity to distribute to peripheral issues. However, the results of pharmacokinetic study were inadequate to justify this assumption. Further studies on tissue distribution and in-depth pharmacokinetics are planned.

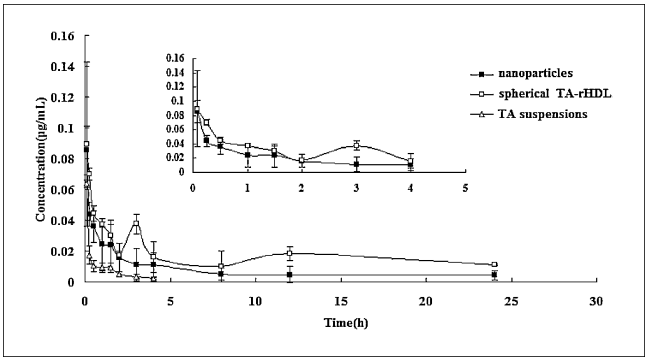

Fig. 3: Mean plasma concentration-time curves of TA after i.v. TA suspensions, nanoparticles (spherical TA-rHDL without apos) and spherical TA-rHDL (578 μg/kg body weight). n = 6, mean ± S.D.

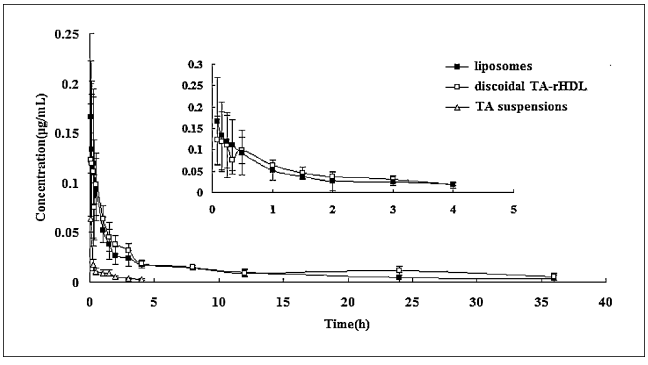

Fig. 4: Mean plasma concentration-time curves of TA after i.v. TA suspensions, liposomes (discoidal TA-rHDL without apos) and discoidal TA-rHDL (578 μg/kg body weight). n = 6, mean ± S.D.

3. Experimental

3.1. Materials

Tanshinone IIA (98% pure) was purchased from Xi'an honson biotechnology Co., Ltd. (China). Lipoid S 100 was obtained from Lipoid GmbH (Germany). Cholesterol and cholesteryl oleate were purchased from Sigma-Aldrich Chemie GmbH and Alfa Aescar/Johnson Matthey Co., Ltd., respectively. Glycerol trioleate was product of Tokyo Kasei Kogyo Co., Ltd. (Japan). The whole apos (97% pure) in HDL with 59% as apoA-I were isolated from the industrial waste during production of albumin in our laboratory. RAW 264.7 cells were obtained from American Type Culture Collection. Very low density lipoproteins were prepared by ultracentrifugation in our laboratory. Oxidized low density lipoproteins of human origin were purchased from Yuanyuan Biotechnology (Guangzhou, China). Lipid-free BSA (A2000) was supplied by APPLYGEN Technologies (Beijing, China). Pancrelipase was obtained from Sigma-Aldrich (L3126). β-Mercaptoethanol were purchased from Sigma-Aldrich. All other reagents used in this study were of analytical grade except methanol of chromatographic grade.

3.2. Animals

Healthy male New Zealand rabbits (body weight 2.0 ± 0.9 kg) were purchased from the Experimental Animal Center of China Pharmaceutical University (Nanjing, China). Prior to the experiments, the rabbits were housed in a temperature and humidity controlled room (23 °C, 55% air humidity) with free access to water and standard rabbits chow. The rabbits were acclimated for at least 5 days and fasted overnight but supplied

with water before the experiments. All experiments were approved by the Institutional Animal Care and Use Committee of China Pharmaceutical University.

3.3. Preparation of drug-loaded spherical and discoidal TA-rHDL

The preparation process for spherical TA-rHDL consisted of construction of the nanoparticles (spherical TA-rHDL without apos) and subsequently incubation with apos. The discoidal ones consisted of construction of the liposomes (discoidal TA-rHDL without apos) and subsequently incubation with apos.

The TA nanoparticles were prepared by a nanoprecipitation/solvent diffusion method as previously described (Zhang et al. 2010a) except that sodium cholate was added in the water phase to mediate later coupling with proteins. Briefly, tanshinone IIA (0.005 g), cholesteryl oleate (> 97% pure, 29% w/w, 0.06 g), glycerol trioleate (> 80% pure, 13% w/w, 0.027 g) and cholesterol (> 95% pure, 6% w/w, 0.012 g) were dissolved in acetone (8 ml) by sonication (DL-720, Shanghai, China), then soybean lecithin (> 97% pure, 46% w/w, 0.1 g) dissolved in 2 ml of absolute ethanol was added to acetone to form an organic phase maintained at $60 \pm 2\,^{\circ}C$. Then the organic phase was injected slowly into an aqueous phase of the same temperature, which contains 0.005 g of sodium cholate, 0.1 M KC1, 1 mM EDTA and 0.01 M Tris-HCl, pH 8.0 in double distilled water (30 ml). Then a semi-transparent pre-emulsion was obtained under constant magnetic agitation. After ultrasonication using an Ultrahomogenizer (JY 92II, Ningbo, China), the dispersion was transferred to a rotary evaporator to remove the organic solvent at 65 °C under reduced pressure. The dispersion was then filtered through 0.22 μm filters to remove larger particles and the filtrate was dialyzed to remove the free sodium cholate using dialysis bags (MW cut off 14,000 Da).

Thin-film dispersion method was alternatively employed to prepare TA liposomes. Briefly, TA (0.005 g), soy lecithin (0.1 g), cholesterol (0.02 g) and sodium cholate (0.005 g) were dissolved in 10 mL of dehydrated alcohol and dried in an eggplant-shaped flask. 15 mL of 0.01 M tris buffer (0.1 M KC1, 1 mM EDTA, pH 8.0) was added, then the mixture was vortexed thoroughly for 5 min, followed by ultrasonication for 300 s using an Ultrahomogenizer (JY 92II, Ningbo, China) until a clear suspension was obtained. The dispersion was then filtered through 0.22 μm filters to remove larger particles and the filtrate was dialyzed to remove the free sodium cholate using dialysis bags (MW cut off 14,000 Da).

The nanoparticles and liposomes obtained above were incubated with the apos to form different TA-rHDL. TA nanoparticles were incubated with apos (7 mg/mL) under 600 rpm stirring at 37 °C for 8 h to form spherical TA-rHDL. Discoidal TA-rHDL were prepared by incubating TA liposomes with apos (7 mg/mL) at low temperature instead (4 °C) for 8 h to ensure their intact structures.

3.4. Measurement of size and zeta potential

Size and zeta potential of spherical and discoidal TA-rHDL with or without apos were measured with dynamic light scattering (DLS) using a Zetasizer 3000 HSA (Malvern, U.K.). Samples were diluted appropriately with aqueous phase prior to the measurements.

3.5. Secondary structures of apolipoproteins

The secondary structures of apos in the lipid-free and lipid-bound forms were determined by circular dichroism (CD) spectroscopy with a Jasco J-810 spectropolarimeter (Japan), between 240 and 190 nm, in a 0.1 cm path length quartz cell at room temperature. Solutions of apos, spherical and discoidal TA-rHDL with protein concentration around 0.05 mg/mL were prepared in tris buffer and dialyzed extensively against 0.005 M sodium tetraborate, pH 10, before CD spectra were recorded. All spectra reported were the average of three individual spectra and have been corrected for baseline contributions from nanoparticles or liposomes. α-Helix, β-structure (β sheet and β turn) and random coil were estimated using a protein secondary structure estimation program (model JWSSE-480, Jasco Corporation) based on the method reported by Yang (Colowick et al. 1986).

3.6. Phagocytosis tests

Mouse macrophage cell line RAW264.7 and foam cell derived from macrophage were employed to study the targeting mechanism of TA-rHDL with different structures.

3.6.1. Cell culture

Mouse macrophage cell line RAW 264.7 were routinely cultured in Dulbecco's Modified Eagle Medium (DMEM) (Sigma, St Louis, USA) containing 10% fetal bovine serum with penicillin (100 U/mL) and streptomycin (100 pg/mL) at 37 °C in humidified, 5% CO_2, 95% air. The macrophage cells were seeded in 24-well tissue culture plates at 1×10^5 cells/well. To obtain foam cells, the macrophage cells were treated with 100 μg/mL oxidized low density lipoproteins (ox-LDL) for 24 h (Xie et al. 2009). Fluorescence microscopic examination of these macrophages revealed a significant accumulation of oil red O in the cells, indicative of lipid accumulation and formation of foam cells.

3.6.2. Plasmid amplification and foam cell transfection

Plasmid DNAs expressing human cholesteryl ester transfer protein (CETP) were amplified in DH-5α *Escherichia coli* and purified using a Genomic DNA kit (Tiangen Biotech). Then foam cells were transfected with plasmid using LipofectAMINE^{TM} LTX reagent (Invitrogen, Carlsbad, CA). Twenty-four hours after the transfection, the cells expressing CETP were used for phagocytic uptake experiment.

3.6.3. Quantification of phagocytic uptake

For spherical TA-rHDL, the roles of apos and very low density lipoproteins (VLDL) were both investigated. Specifically, spherical TA-rHDL with and without apos (30 μg/mL, calculated by the TA content, 200 μL) were added to transfected foam cells expressing CETP or macrophages in the presence of lipid-free BSA (5 mg/mL) and β-mercaptoethanol (4 mM), respectively. In foam cell model, very low density lipoproteins (2 mg/mL, 200 μL) were added as giver of interchangable lipids under the action of CETP to explore phagocytosis mechanism, followed by direct treatment by pancrelipase (80 mIU/mL). For discoidal TA-rHDL, the role of VLDL and LCAT were investigated. Specifically, discoidal TA-rHDL were added to macrophages and transfected foam cells expressing CETP, respectively. In foam cell model, VLDL (2 mg/mL, 200 μL) were added as giver of interchangable lipids under the action of CETP. LCAT were investigated as a promoter for structure changes of discoidal TA-rHDL during phagocytosis.

After an incubation periods of 1, 2 and 3 h respectively, cells were washed three times with D-PBS to remove the non-phagocytosed drug. The washed cells were subject to five cycles of freezing (−40 °C) and thawing (37 °C) to split before dissolved in methanol (100 μL/well). The drug uptake was determined by analyzing the TA in the supernatant using HPLC as described previously (Zhang et al. 2010). The experiments were performed in triplicate.

3.7. Pharmacokinetics studies

3.7.1. Pharmacokinetic design

All studies on animals were in accordance with the guidelines of the Ethics Committee by the university. Thirty rabbits were randomly divided into 5 groups. Spherical and discoidal TA-rHDL, nanoparticles (spherical TA-rHDL without apos), liposomes (discoidal TA-rHDL without apos), and TA suspensions (6 mg TA dissolved in 30 mL water and 15 mL propanediol solution containing 2% dimethyl sulfoxide and 0.9% sodium chloride) were selected for the study. On the day of the experiment, the same dose of TA in 5 different formulations (0.5 mg/kg) was injected through auricular vein. Time taken for administration was 30 s. Blood samples (1 mL) were collected from auricular vein initially and at 5, 15, 30, 60 min and 1.5, 2, 3, 4, 8, 12, 24, 36 h after intravenous injection. Plasma was separated by centrifugation at 3000 rpm for 10 min and stored at − 20 °C until analysis.

3.7.2. Plasma sample preparation

Prior to extraction, frozen plasma samples were thawed at ambient temperature. Sample preparation was carried out under subdued light. A total of 200 μL of rabbit plasma was pipetted in a 10 mL conical centrifuge tube. A single step precipitation protein procedure was adopted to extract TA from rabbit plasma. Firstly, 400 μL acetonitrile was added and vortex-mixed for 3 min to fully precipitate protein. Secondly, the mixture was centrifuged at 3000 rpm for 10 min. Then the supernatant was transferred to a clean centrifuge tube and dried under a stream of nitrogen at 40 °C water bath. The residue was reconstituted with 200 μL of mobile phase and centrifuged at 12000 rpm for 10 min. Aliquots (20 μL) of the supernatant were injected into the HPLC system for analysis.

3.7.3. Chromatographic system

Concentrations of TA was quantified by HPLC (Shimadzu LC-20A, Kyoto, Japan) equipped with a diode array detection (DAD) set at 268 nm (Zhang et al. 2009). The separation was performed at 30 °C on a Synergi Hydro-RP C18 column (5 μm, 250 mm × 4.6 mm, Phenomenex, USA) protected by a C18 Securityguard column (5 μm, 10 mm × 4.6 mm, Kromasil, Sweden). The mobile phase was methanol/water (90:10, v:v), and delivered at a flow rate of 1.0 mL/min. The injection volume was 20 μL.

3.7.4. Method validation

The standard curve for TA was satisfactorily described by 1/x weighted least-squares linear regression. The concentration range was from 5 ng/mL to 500 ng/mL. The linear regression equation was:

$$A = 175264 \times C + 324.5(n = 3,\ r = 0.9976) \quad (1)$$

The limit of quantification was 10 ng/mL. Intra-day and inter-day variabilities were below 10%. No significant matrix effect was observed for the analytes in the plasma samples. All of the absolute recoveries were above 80%, with all RSD less than 10%, which were within the acceptable limits to meet the guidelines for bioanalytical methods.

3.8. Statistics and pharmacokinetic analysis

Data reported were arithmetic mean values ± standard deviations ($\bar{x} \pm$ S.D.). Statistically significant differences were determined using two-tailed student's t-test (SPSS, version 10.0) with $p < 0.05$ or $p < 0.01$ as a level of significance. Pharmacokinetic parameters (± S.D.) were calculated using the software program PKSolver (Zhang et al. 2007; 2010b). Statistical comparisons between groups were performed by an overall analysis of variance with multiple-dependent measures to the 6 calculated pharmacokinetic parameters (between: formulations-within: parameters in a 5 × 6 design) for the 5 different TA formulations.

Acknowledgements: This study is financially supported by the Major Project of National Science and Technology of China for New Drugs Development (No. 2009ZX09310-004) and the National Science Foundation Grant of China (No. 81072587). We thank Professor Hong-wen Zhou (Department of Endocrinology, Jiangsu Province Hospital) for his kind gift of CETP plasmid. We would like to acknowledge the invaluable assistance of Tonrol Bio-Pharmaceutical Co., Ltd. by providing raw material for isolation of apolipoproteins.

References

Ajees A, Anantharamaiah G, Mishra V, Hussain M, Murthy H (2006) Crystal structure of human apolipoprotein AI: insights into its protective effect against cardiovascular diseases. Proc Nat Acad Sci USA 103: 2126–2131.

Angelin B, Parini P, Eriksson M (2002) Reverse cholesterol transport in man: promotion of fecal steroid excretion by infusion of reconstituted HDL. Atheroscler Suppl 3: 23–30.

Assmann G, Nofer J (2003) Atheroprotective effects of high-density lipoproteins. Medicine 54: 321–341.

Barter P, Nicholls S, Rye K, Anantharamaiah G, Navab M, Fogelman A (2004) Antiinflammatory properties of HDL. Circ Res 95: 764–772.

Bobryshev Y (2006) Monocyte recruitment and foam cell formation in atherosclerosis. Micron 37: 208–222.

Bunjes H, Koch MHJ, Westesen K (2003) Influence of emulsifiers on the crystallization of solid lipid nanoparticles. J Pharm Sci 92: 1509–1520.

Chu MQ, Gu HC, Liu GJ (2002) Study on the preparation of tanshinone proliposomes by spray drying method. Zhongguo Yao Xue Za Zhi 37: 32–35.

Collet X, Tall A, Serajuddin H, Guendouzi K, Royer L, Oliveira H, Barbaras R, Jiang X, Francone O (1999) Remodeling of HDL by CETP *in vivo* and by CETP and hepatic lipase *in vitro* results in enhanced uptake of HDL CE by cells expressing scavenger receptor BI. J Lipid Res 40: 1185–1193.

Feng M, Cai Q, Huang H, Zhou P (2008) Liver targeting and anti-HBV activity of reconstituted HDL-acyclovir palmitate complex. Eur J Pharm Biopharm 68: 688–693.

Feng M, Pan S, Zhang J, Wang Q, Wu W, Li R (2005) In vitro phagocytic uptake of PEG-PBLG nanoparticles containing amphotericin B. J China Pharm Univ 36: 321–325.

Fitzgerald M, Mujawar Z, Tamehiro N (2010) ABC transporters, atherosclerosis and inflammation. Atherosclerosis 211: 361–370.

Francone O, Gurakar A, Fielding C (1989) Distribution and functions of lecithin: cholesterol acyltransferase and cholesteryl ester transfer protein in plasma lipoproteins. Evidence for a functional unit containing these activities together with apolipoproteins AI and D that catalyzes the esterification and transfer of cell-derived cholesterol. J Biol Chem 264: 7066–7022.

Frank P, Marcel Y (2000) Apolipoprotein AI: structure-function relationships. J Lipid Res 41: 853–872.

Han F, Li S, Yin R, Liu H, Xu L (2008) Effect of surfactants on the formation and characterization of a new type of colloidal drug delivery system: Nanostructured lipid carriers. Colloids Surf A Physicochem Eng Asp 315: 210–216.

Hao H, Wang G, Cui N, Li J, Xie L, Ding Z (2007) Identification of a novel intestinal first pass metabolic pathway: NQO1 mediated quinone reduction and subsequent glucuronidation. Curr Drug Metab 8: 137–149.

Herbert PN, Bernier DN, Cullinane EM, Edelstein L, Kantor MA, Thompson PD (1984) High-density lipoprotein metabolism in runners and sedentary men. JAMA 252: 1034–1037.

Hiltunen T, Luoma J, Nikkari T, Yla-Herttuala S (1998) Expression of LDL receptor, VLDL receptor, LDL receptor-related protein, and scavenger receptor in rabbit atherosclerotic lesions: marked induction of scavenger receptor and VLDL receptor expression during lesion development. Circulation 97: 1079–1086.

Jonas A, Wald J, Toohill K, Krul E, Kezdy K (1990) Apolipoprotein AI structure and lipid properties in homogeneous, reconstituted spherical and discoidal high density lipoproteins. J Biol Chem 265: 22123–22129.

Joshi M, Pathak S, Sharma S, Patravale V (2008) Design and *in vivo* pharmacodynamic evaluation of nanostructured lipid carriers for parenteral delivery of artemether: Nanoject. Int J Pharm 364: 119–126.

Kontush A, Chapman MJ (2006) Functionally defective high-density lipoprotein: a new therapeutic target at the crossroads of dyslipidemia, inflammation, and atherosclerosis. Pharmacol Rev 58: 342–374.

Lacko A, Nair M, Paranjape S, Johnson S, McConathy W (2002) High density lipoprotein complexes as delivery vehicles for anticancer drugs. Anticancer Res 22: 2045–2049.

Lehrer S (1971) Solute perturbation of protein fluorescence. Quenching of the tryptophyl fluorescence of model compounds and of lysozyme by iodide ion. Biochemistry 10: 3254–3263.

Li H, Zhang Z, Ma L, Chen X (2007) Preparation of tanshinone microemulsion and its absorption in rat intestine in situ. Zhongguo Zhong Yao Za Zhi 32: 1024–1027.

Li P, Wang GJ, Li J, Hao HP, Zheng CN (2006) Characterization of metabolites of tanshinone IIA in rats by liquid chromatography/tandem mass spectrometry. J Mass Spectrom 41: 670–684.

Li Q, Wang Y, Feng N, Fan Z, Sun J, Nan Y (2008) Novel polymeric nanoparticles containing tanshinone IIA for the treatment of hepatoma. J Drug Target 16: 725–732.

Liang L, Chen Y, Xiong S, Zeng Z, Sun M, Zhang H (2007) The inhibitive effect produced by local perfusion of tanshinone IIA nanoparticle on neointimal hyperplasia of rabbit carotid artery following intimal denudation. Sheng Wu Yi Xue Gong Cheng Xue Za Zhi 24: 812–816.

Liang Z, Mao S, Yin Z, Jin H, Li H, Chu T (2008) Preparation and quality evaluation of intravenous tanshinone II (A) emulsion. Zhongguo Zhong Yao Za Zhi 33: 1249–1252.

Libby P, Bonow R, Mann D, Zipes D (2008) Braunwald's heart disease: A textbook of cardiovascular medicine, 8th ed., Saunders Elsevier: Philadelphia, PA.

Linsel-Nitschke P, Tall A (2005) HDL as a target in the treatment of atherosclerotic cardiovascular disease. Nat Rev Drug Discov 4: 193–205.

Liu J, Zhu J, Du Z, Qin B (2005) Preparation and pharmacokinetic evaluation of Tashinone IIA solid lipid nanoparticles. Drug Dev Ind Pharm 31: 551–556.

Lou B, Liao X, Wu M, Cheng P, Yin C, Fei Z (2005) High-density lipoprotein as a potential carrier for delivery of a lipophilic antitumoral drug into hepatoma cells. World J Gastroenterol 11: 954–959.

Mahley R, Innerarity T (1983) Lipoprotein receptors and cholesterol homeostasis. Biochim Biophys Acta 737: 197–222.

Marier JF, Vachon P, Gritsas A, Zhang J, Moreau JP, Ducharme MP (2002) Metabolism and disposition of resveratrol in rats: extent of absorption, glucuronidation, and enterohepatic recirculation evidenced by a linked-rat model. J Pharmacol Exp Ther 302: 369–373.

Massey J, Gotto A (1979) Contribution of alpha helix formation in human plasma apolipoproteins to their enthalpy of association with phospholipids. J Bioll Chem 254: 9559–9561.

McConathy W, Nair M, Paranjape S, Mooberry L, Lacko A (2008) Evaluation of synthetic/reconstituted high-density lipoproteins as delivery vehicles for paclitaxel. Anticancer Drugs 19: 183–188.

McGuire KA, Davidson WS, Jonas A (1996) High yield overexpression and characterization of human recombinant proapolipoprotein AI. J Lipid Res 37: 1519–1528.

Ogino C, Shibata N, Sasai R, Takaki K, Miyachi Y, Kuroda S, Ninomiya K, Shimizu N (2010) Construction of protein-modified TiO_2 nanoparticles for use with ultrasound irradiation in a novel cell-injuring method. Bioorg Med Chem Lett 20: 5320–5325.

Phillips J, Wriggers W, Li Z, Jonas A, Schulten K (1997) Predicting the structure of apolipoprotein AI in reconstituted high-density lipoprotein disks. Biophys J 73: 2337–2346.

Rensen P, Vrueh, R, Kuiper J, Bijsterbosch M, Biessen E, Berkel T (2001) Recombinant lipoproteins: lipoprotein-like lipid particles for drug targeting. Adv Drug Deliv Rev 47: 251–276.

Pownall H, Gotto A (1992) Human plasma apolipoproteins in biology and medicine. Structure and Function of Apolipoproteins 1–32.

Saito H, Dhanasekaran P, Nguyen D, Deridder E, Holvoet P, Lund-Katz S, Phillips M (2004) α-Helix formation is required for high affinity binding of human apolipoprotein AI to lipids. J Biol Chem 279: 20974–20981.

Schöler N, Hahn H, Müller R, Liesenfeld O (2002) Effect of lipid matrix and size of solid lipid nanoparticles (SLN) on the viability and cytokine production of macrophages. Int J Pharm 231: 167–176.

Scherphof G, Roerdink F, Waite M, Parks J (1978) Disintegration of phosphatidylcholine liposomes in plasma as a result of interaction with high-density lipoproteins. Biochim Biophys Acta 542: 296–307.

Skajaa T, Cormode D, Jarzyna P, Delshad A, Blachford C, Barazza A, Fisher E, Gordon R, Fayad Z, Mulder W (2010) The biological properties of iron oxide core high-density lipoprotein in experimental atherosclerosis. Biomaterials 32: 206–213.

Song X, Fischer P, Chen X, Burton C, Wang J (2009) An apoA-I mimetic peptide facilitates off-loading cholesterol from HDL to liver cells through scavenger receptor BI. Int J Biol Sci 5: 637–646.

Su ZR, Liu ZQ, Zhou H (1997) Change of chemical composition of tashinone in concentration and drying technology (1) degradation mechanism of Tashinone IIA under the heat and moisture. Chin Trad Patent Med 19: 5–6.

Thomas M, Bhat S, Sorci-Thomas M (2008) Three-dimensional models of HDL apoA-I: implications for its assembly and function. J Lipid Res 49: 1875–1883.

Vaisar T, Pennathur S, Green P, Gharib S, Hoofnagle A, Cheung M, Byun J, Vuletic S, Kassim S, Singh P (2007) Shotgun proteomics implicates protease inhibition and complement activation in the antiinflammatory properties of HDL. J Clin Investig 117: 746–756.

Xie S, Lee Y, Kim E, Chen L, Ni J, Fang L, Liu S, Lin S, Abe J, Berk B (2009) TR4 nuclear receptor functions as a fatty acid sensor to modulate CD36 expression and foam cell formation. Proc Nat Acad Sci 106: 13353–13358.

Yang JT, Wu CSC, Martinez HM. In: Colowick S, Kaplan N, Hirs C, Timasheff S (1986) Methods in enzymology: Enzyme structure: Part K: Academic Press; 130: 208–269.

Zannis V, Chroni A, Krieger M (2006) Role of apoA-I, ABCA1, LCAT, and SR-BI in the biogenesis of HDL. J Mol Med 84: 276–294.

Zhang Y, Zhou JP, Huo MR (2007) A data analysis program in pharmacokinetics base on Microsoft Excel-Development and validation of PKSlover 1.0. J Math Med 20: 58–61.

Zhang W, Gu X, Bai H, Yang R, Dong C, Liu J (2010a) Nanostructured lipid carriers constituted from high-density lipoprotein components for delivery of a lipophilic cardiovascular drug. Int J Pharma 391: 313–321.

Zhang W, Liu J, Liu X, Chen Z (2009) Stealth tanshinone IIA-loaded solid lipid nanoparticles: effects of poloxamer 188 coating on in vitro phagocytosis and *in vivo* pharmacokinetics in rats. Yao Xue Xue Bao 44: 1421–1428.

Zhang Y, Huo M, Zhou J, Xie S (2010b) PKSolver: An add-in program for pharmacokinetic and pharmacodynamic data analysis in Microsoft Excel. Comput Methods Programs Biomed 99: 306–314.

Zhao BL, Jiang W, Zhao Y, Hou JW, Xin WJ (1996) Scavenging effects of salvia miltiorrhiza on free radicals and its protection for myocardial mitochondrial membranes from ischemia-reperfusion injury. Biochem Mol Biol Int 38: 1171–1182.